ACS APPLIED NANO MATERIALS
Cite This: ACS Appl. Nano Mater. 2019, 2, 1045−1052
Article
www.acsanm.org

Strong Purcell Effect for Terahertz Magnetic Dipole Emission with Spoof Plasmonic Structure

Hong-Wei Wu,*[,†,‡] Yang Li,*[,†] Hua-Jun Chen,[†] Zong-Qiang Sheng,[†] Hao Jing,[‡] Ren-Hao Fan,[‡] and Ru-Wen Peng[‡]

[†]School of Mechanics and Photoelectric Physics, Anhui University of Science and Technology, Huainan 232001, China
[‡]National Laboratory of Solid State Microstructures, School of Physics, and Collaborative Innovation Center of Advanced Microstructures, Nanjing University, Nanjing 210093, China

ABSTRACT: The magnetic Purcell effect is usually described as a modification of the magnetic dipole emission with a resonator. In an optical spectrum, various metallic and dielectric structures have been proposed to enhance the magnetic dipole emission. However, the enhancement of magnetic dipole emission by a well-designed structure has not been extensively investigated in the terahertz spectrum. Here, we propose a spoof plasmonic structure to enhance strongly the magnetic dipole emission by controlling the electromagnetic environment in the terahertz spectrum. The spoof plasmonic structure with deep-subwavelength scale is designed by periodically inserting metallic strips into a hollow silicon cylinder to obtain the "hot spot" of the localized magnetic field in the structural hollow. The resonant frequency and intensity of the magnetic dipole mode supported in this structure can be tuned freely by tailoring the structural parameters. In this context, we investigate the enhancement of a magnetic dipole emission by putting a magnetic dipole at the hollow of the spoof plasmonic structure. The results indicate that the Purcell factor can be more than 10^3 for a magnetic dipole emission, which is 1 order of magnitude larger than the hollow bare silicon cylinder case. We furthermore investigate the dependence of the Purcell factor on the structural parameters. The spoof plasmonic structure provides the unique ability to enhance the emission from terahertz magnetic dipoles, opening new avenues for novel magnetic light-matter interactions in the terahertz region.

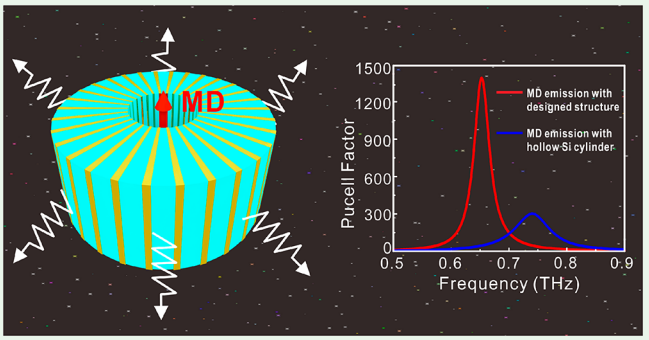

KEYWORDS: *spoof plasmonic structure, metamaterials, magnetic resonances, Purcell effect, emission enhancement*

INTRODUCTION

The interaction between light and matter is widely considered to be solely mediated by the electric field, since it is suggested that magnetic dipole (MD) transitions are very weak in nature compared to electric dipole (ED) transitions based on the Bohr model.[1] Nevertheless, manipulating the magnetic component of light plays the same crucial role as the electric component in the realization of exotic optical phenomenon.[2−5] In this context, enhancing MD emissions by controlling the electromagnetic environment is of great significance for various fundamental researches and applications. In nature, the lanthanide series ions Eu^{3+} can support relatively stronger MD transitions in the visible band. To realize the enhancement of MD emissions, various plasmonic nanostructures have been exploited to provide a large magnetic local density of states (MLDOS) for modifying the electromagnetic environment of the emitter.[6−10] However, the intrinsic Ohmic losses in plasmonic nanostructures inevitably lead to low quantum efficiency and limit the enhancement of MD emission. High-index dielectric nanostructures which support inherently strong MD resonances at optical frequency with low absorption losses in the visible spectrum are promising candidates for MD emission enhancement.[11−19] For example, a hollow silicon (Si) disk has been proposed to enhance MD emission, and the Purcell factor (PF) can be more than 300.[13,14] Furthermore, it has been reported that for the rare-earth ions, such as Er^{3+} ions, that the magnetic dipole transitions can have selective ultrafast excitation and emission in $ErFeO_3$ at the terahertz (THz) band.[20] Certainly, it is unambiguous that enhancing the MD emission in the THz frequencies can be achieved by using high-index dielectric structures according to the scaling rule. However, the dielectric structures cannot provide a stronger localized magnetic field to achieve further emission enhancement due to large radiation losses. It is important that a strong Purcell effect of THz magnetic dipole emission can be realized by enhancing the localized magnetic field intensity in the resonator, facilitating various applications, such as THz Raman scattering enhancement, THz laser, THz sensors, etc.

Moreover, to obtain the localized field enhancement in the THz region, the concept of spoof localized surface plasmons

Received: December 20, 2018
Accepted: January 22, 2019
Published: January 22, 2019

DOI: 10.1021/acsanm.8b02318
ACS Appl. Nano Mater. 2019, 2, 1045−1052

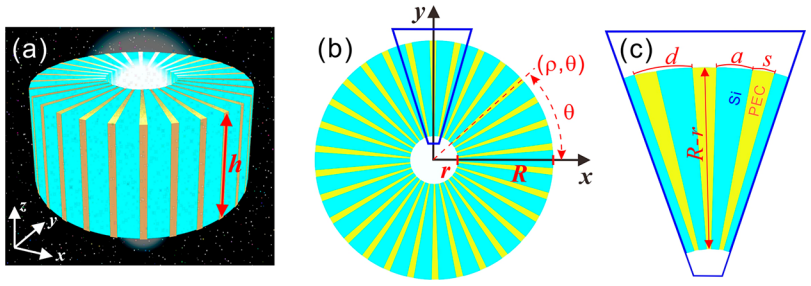

Figure 1. (a) Schematics of the proposed spoof plasmonic structure with high *h*. (b) Two-dimensional cross-section view of the spoof plasmonic structure with inner radius r, outside radius R. Cyan and yellow regions represent the Si and metal materials. (c) Schematic of the structural parameters by enlarging the blue region in (b). Period, slit width, metallic width, and metallic length are *d*, *a*, *s*, and $R - r$, respectively.

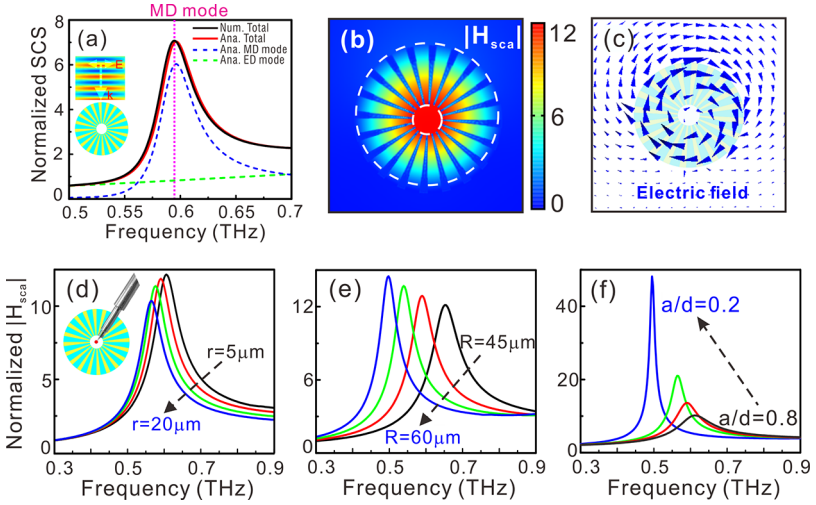

Figure 2. (a) The calculated SCS spectrum for the spoof plasmonic structure. Black solid line denotes the simulated result and red solid line is the analytic calculation. Blue and green dash lines correspond to the SCS of the MD and ED resonant modes. Vertical pink dotted line denotes the frequency of MD resonance. (b) The distribution of the ormalized magnetic field $|H_{sca}|$ at the resonant frequency of MD mode in the spoof plasmonic structure. (c) The distribution of electric field denoted as blue arrows. (d–f) Normalized $|H_{sca}|$ calculated at the center of the spoof plasmonic structure as a function of frequency for different inner radiuses *r*, outside radiuses *R*, and ratios *a*/*d*. The inset in panel d indicates the location of the alculated magnetic field intensity $|H_{sca}|$ at the red point.

(LSPs) based on the textured perfect electric conductor (PEC) cylinder has been proposed to mimic the metallic nanoparticles supporting the LSPs in optical frequencies.[21] Since then, extensive theoretical and experimental works have been performed to verify the existence of spoof LSPs in various textured metallic structures[22−28] which can localize the electric field. Particularly, a three-dimensional textured PEC cylinder with finite thickness has also been experimentally demonstrated to support not only electric LSPs, but also magnetic LSPs at deep subwavelength volumes.[29] However, the maximum magnetic field of the magnetic LSPs in the solid textured metal cylinder is confined inside the structure and inaccessible to nearby MD emitters for terahertz MD emission enhancement. Recently, we also have demonstrated that a hollow metallic cylinder with periodic cut-through slits can support the magnetic and electric dipole resonances similar to the Mie-resonances in dielectric particles with a high-refractive index.[30,31] However, this structure has a greater freedom degree for tuning resonant response by changing the geometry parameters compared with natural high-index dielectric particles. Furthermore, as compared with the solid spoof plasmonic structure, the hollow structure has a prominent ability to localize the maximal magnetic field in the hollow by tailoring the structural parameters, and it may provide a versatile platform to enhance the THz magnetic dipole emission with a high Purcell factor.

In this paper, we demonstrate that the hollow spoof plasmonic structure can greatly enhance the magnetic field intensity in the structural hollow to modify the electromagnetic environment of the magnetic dipole emitter for achieving the strong Purcell effect at the THz frequency range. The structure is designed by periodically inserting metallic strips into a hollow silicon cylinder with a deep subwavelength scale. The resonant frequency and localized magnetic field intensity of the MD resonance in the spoof plasmonic structure can be tuned freely by tailoring the geometric parameters of the structure. Particularly, the ability of focusing a magnetic field can be significantly improved by increasing the number and width of the metallic strips. On the basis of this ability, we investigate the magnetic Purcell effect by putting the MD emitter into the center of the structure. The results indicate that the Purcell factor can be more than 10^3 for MD emission, which is 1 order of magnitude larger than the Purcell factor of a bare hollow Si cylinder with the same structural scale. Furthermore, it is also studied how the geometry of the spoof Plasmonic structure affects the enhancement of MD emission. Importantly, the structure is unique to modify strongly the emission of a magnetic THz source at a deep subwavelength scale, opening up new exciting possibilities in magneto-optics.

DOI: 10.1021/acsanm.8b02318
ACS Appl. Nano Mater. 2019, 2, 1045−1052

RESULTS AND DISCUSSION

The proposed spoof plasmonic structure is schematically shown in Figure 1a. The structure is designed by periodically inserting metallic strips into a hollow Si cylinder with height h, inner radius r, and outside radius R. The $x-y$ cross section of the structure is shown in Figure 1b, and (ρ, θ) are the polar coordinates. The length and width of metallic strips are $R - r$ and s, the width of dielectric Si in slits is a, then period $d = a + s = 2\pi R/N$, where N is the number of metallic strips. These structural parameters are illustrated in detail in Figure 1c by enlarging the blue region of Figure 1b for clarity. The hollow Si cylinder is decorated only in the $x-y$ plane by inserting periodic metallic strips. It is well-known that the strong localized magnetic field intensity is needed for enhancement of the MD emission. Thus, we first examine the scattering property and the localization of the magnetic field in the spoof plasmonic structure for plane-wave excitation in the two-dimension (2D) scenario. It is indicated in the inset of Figure 2a that the plane-wave with H_z polarization occupies the structure from top to bottom. As a start point, we take the spoof plasmonic structure with the number of metallic strips $N = 20$, outside radius $R = 50$ μm, inner radius $r = 10$ μm, and the ratio between slit and period $a/d = 0.4$ in the azimuthal direction. For proof-of-principle purposes, we assume the metallic strips as made of a PEC in the terahertz frequency. In order to investigate the electromagnetic resonant modes supported by the spoof plasmonic structure, we conduct full-wave simulations for plane wave excitation based on finite element analysis with COMSOL Multiphysics.

In Figure 2a, we obtain the scattering cross-section (SCS) by integrating the scattering power on a hypothetical 2D circle enclosing the structure and normalizing to incident irradiation and the structural parameter R. As shown in Figure 2a with the black solid line, a magnetic dipole resonance can be clearly found at 0.595 THz in normalized SCS. To gain a deeper insight into the magnetic dipole resonant response of spoof plasmonic structure, we also present an analytical equation for the scattering cross section of the spoof plasmonic structure by applying the concept of an electromagnetic metamaterial. It is well-known that the structure can also be regarded as a hollow metamaterial cylinder with thickness $R - r$ for the transverse-magnetic (TM) polarized incident wave, and the effective parameters of the metamaterial can be expressed as[21]

$$\varepsilon_r = \begin{bmatrix} -\infty & 0 & 0 \\ 0 & n_{Si}^2 d/a & 0 \\ 0 & 0 & -\infty \end{bmatrix}, \quad \mu_r = \begin{bmatrix} a/d & 0 & 0 \\ 0 & \infty & 0 \\ 0 & 0 & a/d \end{bmatrix} \tag{1}$$

where the refractive index of silicon is chosen as $n_{Si} = 3.48$. In internal and external regions of the hollow metamaterial cylinder, Maxwell's equations can be decomposed into the free-space Helmholtz's equation for H_z component. Solving the second order differential equations, the H_z is given by considering the finite energy in internal region and the Sommerfeld radiation conditions in external region, which are shown as[32]

$$H_z(\rho, \theta) = \sum_{m=-\infty}^{\infty} A_m J_m(k_0\rho) \exp(im\theta) \tag{2}$$

in internal region $\rho < r$ and

$$H_z(\rho, \theta) = \sum_{m=-\infty}^{\infty} D_m H_m^{(1)}(k_0\rho) \exp(im\theta) \tag{3}$$

in external region $\rho > R$, where J_m and $H_m^{(1)}$ are the Bessel and Hankel functions of the first kind, respectively. A_m and D_m are complex constants. The parameters m and k_0 are the azimuth index and wave vector of incident light. In metamaterial, since the radial component of permittivity tends to $-\infty$, the magnetic field can be simply written as[31]

$$H_z(\rho, \theta) = \sum_{m=-\infty}^{\infty} (B_m J_0(k_0 n_{Si}\rho) + C_m Y_0(k_0 n_{Si}\rho)) \exp(im\theta) \tag{4}$$

where J_0 and Y_0 are the zero order Bessel functions of the first and second kind, B_m and C_m are complex constants. After matching boundary conditions on H_z and E_θ at inner and outside boundaries ($\rho = r$, $\rho = R$), the analytic expression of the SCS of the spoof plasmonic structure is given as

$$\sigma_{sc} = \frac{4}{k_0} \sum_{m=-\infty}^{\infty} |D_m|^2 \tag{5}$$

The complex constant D_m can be written as

$$D_m = -i^m \frac{\frac{a}{d} p J_m(k_0 R) + q n_{Si} J_m'(k_0 R)}{\frac{a}{d} p H_m^{(1)}(k_0 R) + q n_{Si} H_m^{(1)\prime}(k_0 R)} \tag{6}$$

where $p = J_1(k_0 n_{Si} R) - M Y_1(k_0 n_{Si} R)$, $q = J_0(k_0 n_{Si} R) - M Y_0(k_0 n_{Si} R)$ and $M = [J_m'(k_0 r)\ J_0(k_0 n_{Si} r)/J_m(k_0 r) + a\, J_1(k_0 n_{Si} r)/(n_{Si} d)]/[J_m'(k_0 r)\ Y_0(k_0 n_{Si} r)/J_m(k_0 r) + a\, Y_1(k_0 n_{Si} r)/(n_{Si}\, d)]$. J_0 and J_1 (Y_0 and Y_1) are the zero- and first-order Bessel functions of first (second) kind, respectively. The slanted prime ($'$) means differentiation with respect to the argument in parentheses. In Figure 2a, the analytical normalized total SCS is shown with red solid curve. We can find that they exhibit the same spectra features by comparing the black and red solid curves. It is well-known that $m = 0$, $m = 1$ in eq 5, respectively, correspond to the MD and ED mode,[30] then the analytical SCS can be identified by calculating the SCS of individual resonance mode as shown in blue dash line and green dash line of Figure 2a, respectively. It is obvious that the MD scattering spectrum presents a resonance around 0.595 THz, which dominates the total scattering efficiency over the ED contribution. This conclusion can be further confirmed in Figure 2b, where we show that the scattering field distribution of the MD mode normalized the incident field intensity at the resonant frequency 0.595 THz as marked by the vertical pink dash line of Figure 2a. From the normalized field distribution, it is not difficult to find that the mode distribution exhibits a circular spot pattern for the magnetic field, and the maximum magnetic field intensity is located in the structural hollow. To clarify further the origin of the magnetic dipole mode, we also calculate the electric field distribution in Figure 2c denoted as blue arrows at the resonant frequency. It is indicated that the displacement current along the azimuth direction of the spoof plasmonic structure in the $x-y$ plane is formed to induce the magnetic dipole moment along the z direction.

Next, we investigate the influences of the structural change on the magnetic field intensity probed at the structural center (as the red point in the inset of Figure 2d). In Figure 2d, we can find that the maximum magnetic field spectrum red shifts with an increase of the inner radius from $r = 5$ to 20 μm for the number of metallic strips $N = 20$, outside radius $R = 50$ μm,

DOI: 10.1021/acsanm.8b02318
ACS Appl. Nano Mater. 2019, 2, 1045−1052

and the ratio between slit and period a/d = 0.4 in the azimuthal direction, and the magnetic field intensity is slightly decreased. Similarly, with an increase of the outside radius from R = 45 to 60 μm in Figure 2e for an inner radius r = 10 μm, the resonant frequency corresponding to the MD mode also decreases, while the intensity becomes stronger. In the metamaterial approximation, the shift of resonant frequency of the MD mode can be attributed to the radius change of the displacement current circle excited by the electric field. For instance, the resonant frequency of the MD mode increases with the decrease of outside radius of the structure because the radius of the displacement current circle is inward compressed. Inversely, the radius of the displacement current circle is pushed outward with increasing inner radius of this structure and leads to the redshift of the MD mode as seen in Figure 2d.[31] Astoundingly, when increasing the width of metallic strips, the magnetic field intensity sharply increases in the hollow. For example, the normalized magnetic field intensity at the structural center increases from 12 to 48 for the ratio a/d from 0.8 to 0.2 in Figure 2f. Here, other parameters are set as the number of metallic strips N = 20, outside radius R = 50 μm, and inner radius r = 10 μm. The reason for this phenomenon is that the electromagnetic response of the structure is enhanced due to the increase of the permittivity and decrease of the permeability, which depend linearly on d/a and a/d, respectively. It opens new possibilities to focus the magnetic field and form magnetic "hot spot" by carefully designing the structure.

It is well-known that the number of metallic strips determines the localization of the electromagnetic field, which has been discussed in ref 30 for the localized electric field intensity in spiral geometries. Next, we discuss the influence of the number of metallic strips in the spoof plasmonic structure on the localized magnetic field intensity. Figure 3a shows the structural representation for the number of metallic strips N = 0, 10, 20, 30, from top to bottom. Here, the structural parameters are set as R = 50 μm, r = 10 μm, and $s = 25\pi/9$ μm. It can be seen that the normalized SCS is redshifted and the peak width becomes more narrow with

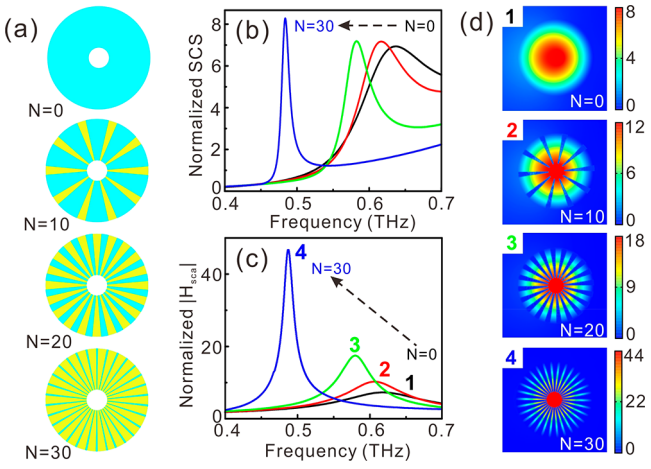

Figure 3. (a) Schematics of the spoof plasmonic structure with different N. (b) Calculated normalized SCS spectrum as a function of frequency. (c) Magnetic field intensity at the structural center as a function of frequency. (d) Magnetic field distributions with the resonant frequencies denoted as "1", "2", "3", "4" in panel c for N = 0, 10, 20, 30.

increasing the number N from 0 to 30 as shown in Figure 3b, while the associated MLDOS increases in the spoof plasmonic structure. This effect stems from the electric field enhancement in the azimuthal direction by increasing the number of metallic strips inserted into the hollow Si cylinder. Since the MLDOS directly relates to the field confinement capabilities of the structure, the magnetic field intensity is enhanced in the hollow with increasing the number N. To confirm this conduction, we calculate the magnetic field intensity at the structural center for the number N from 0 to 30 in Figure 3c. As expected, the normalized field intensity is sharply enhanced from 8 to 44, and the peak width also becomes narrow. The spectrum positions of the maximum magnetic field intensities accurately agree with the positions of resonant MD mode of normalized SCS in Figure 3b. Further, the magnetic field patterns corresponding to the peaks in Figure 3c denoted by "1", "2", "3", and "4" are given in Figure 3d. The images in Figure 3d show the localized magnetic field enhancement with the increase of the metallic strips. It is not difficult to observe that the intensity of the MD mode is further enhanced in the hollow and that the mode volume is further inwardly compressed from the top to bottom of Figure 3d.

Until now, we have demonstrated that the localized magnetic field intensity of the MD mode can be sharply enhanced in the hollow by increasing the width and number of metallic strips inserted in the hollow Si cylinder, which provides the condition of enhanced MD emission when an MD emitter is put into the structural center. As the next step, we investigate the magnetic Purcell effect, which is usually described as a modification of the magnetic dipole emission with a resonator. To evaluate the modification effect of the dipole emission, we calculate the PF, which is defined as the ratio of the magnetic transition decay rate in the modified environment γ and the decay rate in vacuum γ_0. Generally, the decay rate of an emitter can be described by Fermi's golden rule as[10]

$$\gamma = \frac{2\pi}{\hbar^2}\sum_f |\langle f|H_I|i\rangle|^2 \delta(\omega_i - \omega_f) \tag{7}$$

with the initial state $|i\rangle$, the final state $|f\rangle$. The interaction Hamiltonian H_I can be described as $H_I = -\mathbf{p}\cdot\mathbf{E} - \mathbf{m}\cdot\mathbf{B} - \cdots$, where the dots represent further higher order interactions. $\mathbf{p}$ is the electric and $\mathbf{m}$ is the magnetic dipole moment of the emitter. In this paper, we focus on the problem of magnetic dipole emission. Thus, the electric part can be neglected in the interaction Hamiltonian H_I and it is convenient to rewrite eq 7 as[10]

$$\gamma = \frac{\pi\omega}{3\hbar}(\mu_0 |\mathbf{m}|^2 \Lambda(\omega)) \tag{8}$$

where Λ is the MLDOS, which is proportional to the amount of power a magnetic oscillating dipole loses when it is placed at the respective position. Thus, the PF can also be expressed as the ratio of the power lost by an ideal oscillating magnetic dipole with or without the structure:[13,15]

$$\mathrm{PF} = \gamma/\gamma_0 = P/P_0 \tag{9}$$

where P is the power lost from a MD emitter modified with the structure and P_0 is the power lost by a MD emitter in vacuum. In general, the power lost P can be expressed as the sum of far-field radiated power P_{rad} and near-field absorbed power P_{abs}, and the PF can be described as $(P_{rad} + P_{abs})/P_0$. Similarly, the

DOI: 10.1021/acsanm.8b02318
ACS Appl. Nano Mater. 2019, 2, 1045−1052

normalized decay rates of the radiative and absorptive parts can be expressed as $\gamma_{rad}/\gamma_0 = P_{rad}/P_0$ and $\gamma_{abs}/\gamma_0 = P_{abs}/P_0$, responsively. To characterize the far-field radiative efficiency of the MD emitter modified by the spoof plasmonic structure, we also study the extrinsic quantum yield, which is defined as $\eta_{ext} = P_{rad}/(P_{rad} + P_{abs})$ with the assumption of unit intrinsic quantum yield for the sake of simplicity. In this way, the assumption of metal as a PEC with zero loss is no longer valid. Hence, we use the practical material copper (Cu) with the finite losses (the conductivity of Cu is $\sigma = 5.998 \times 10^7$ S/m) to construct the spoof plasmonic structure for investigating the Purcell enhancement of MD emission in the following section. Using the commercial software COMSOL Multiphysics, we calculate the normalized far field radiated power P_{rad} by a MD from the integral of power flow through a closed surface containing the dipole and the structure, while the absorbed power P_{abs} is calculated by the volume integral of power dissipation in the Cu strips of spoof plasmonic structure.

We consider the MD emitter with the magnetic dipole moment parallel to the z-axis in the structural center, as indicated by the red arrow in Figure 4a (The inset at top left corner of Figure 4b also shows the direction of magnetic dipole moment by sketching a half structure for clarity). The structural parameters: outside radius $R = 50$ μm, inner radius $r = 10$ μm, the number of metallic strips $N = 20$, height $h = 100$ μm, and width of metallic strips $s = 25\pi/9$ μm are selected for calculating the PF of MD emission. These size parameters are practical and such structures can be fabricated with the conventional photolithography techniques.[27,28,33] For the terahertz magnetic dipole emitter, such materials $ErFeO_3$,[20] $TmFeO_3$,[34] and $DyFeO_3$[35] that have the strong magnetic dipole transitions might be incorporated via a specific solution to fill the structural hollow as quantum dots in the poly(vinyl alcohol) solution.[36] Furthermore, it needs to be explained that the number of metallic strips is selected as $N = 20$ for easy fabrication of the spoof plasmonic structure in practical applications, even if the structure with $N = 30$ has a stronger ability to confine the localized magnetic field as can be seen in Figure 3d. It is exciting that the PF can attain nearly 1300 at the magnetic dipole resonant frequency of 0.655 THz as can be seen in the red curve of Figure 4b. Here, we can note that the resonant frequency of the MD mode is different with the value $f = 0.595$ THz in Figure 2a because the spoof plasmonic structure changes from 2D to 3D with a decrease in the height from $h = \infty$ to $h = 100$ μm. For comparison, we have also calculated the PF of the same MD located at the center of the hollow bare Si cylinder with the same structure for $N = 0$. The black curve of Figure 4b shows the result that the calculated PF is close to 300 at a resonant frequency of 0.742 THz, which is similar to the optical frequency results of the hollow bare Si disk.[13,14] The right inset in Figure 4b identifies the resonant frequencies of the structure with different number N of metallic strips. Obviously, the PF for the spoof plasmonic structure is far greater than the one for the hollow bare Si cylinder. The reason for the larger PF is that the spoof plasmonic structure can strongly gather the magnetic field and form the magnetic "hot spot" as compared with the bare Si cylinder. Furthermore, the enhancement of the MD emission also can be intuitively understood by introducing an approximate analysis as $\gamma_{rad}/\gamma_0 = P_{rad}/P_0 \approx |\mathbf{m} + \mathbf{m}_{ind}|^2/|\mathbf{m}|^2$,[10] where $\mathbf{m}_{ind}$ is the magnetic dipole moment induced in the spoof plasmonic structure. It can be predicted that the MD emission can be more enhanced by using the spoof plasmonic structure, which has a stronger ability for localizing the magnetic field under the plane wave illumination. In other words, when the MD emitter is in the hollow of the spoof plasmonic structure, the greater dipole moment of the MD mode under the plane wave illumination can further enhance the MD emission. It should be noted that the spoof plasmonic structure also supports the ED mode accompanying the MD mode under the plane wave excitation, although the ED mode contribution to the total scattering is smaller than the MD one as shown in the green dash line of Figure 2a. However, in order to obtain the enhancement of the pure MD emission, the enhancement of ED emission at this resonant frequency needs to be suppressed. Therefore, we also study the PF of an ED located at the center of the spoof plasmonic structure with the electric dipole orientation being parallel to the x axis, as indicated by the inset at the bottom left corner of Figure 4b. The blue dash line shows the PF for the ED emission enhancement by amplifying 50 fold in magnitude, and the PF is less than 1 at around 0.655 THz, actually. In other words, the ED emission is suppressed when the MD is enhanced by using the structure. In fact, it can be understood that the ED emitter locates the position of the minimum electric field intensity at the structural center for the MD resonance, the electric field distribution of which is like doughnut. At the same time, the resonant frequency of the ED mode is far away from the MD resonance. Thus, the ED emission can be negligible at the MD resonance for achieving the pure MD emission enhancement. In Figure 4c, we show the radiation pattern of the far field for the MD mode modified by the spoof

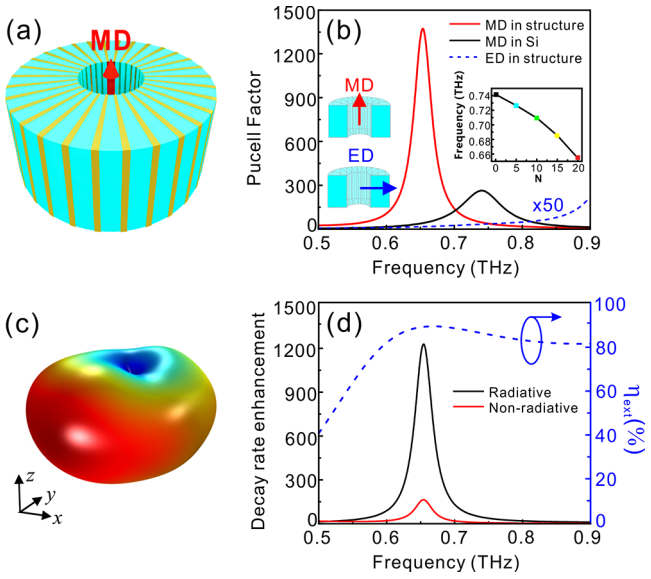

Figure 4. (a) Schematic diagram of spoof plasmonic structure for a MD emitter at the structural center. (b) PF of a MD enhanced by spoof plasmonic structure as shown with red solid line, the black solid line is the PF of a MD enhanced by a hollow bare Si cylinder with same structural scale. Top left inset indicates the direction of magnetic dipole moment. Blue dash line corresponds to the PF of an ED with the same structure by enlarging 50 fold in magnitude. Right inset shows the resonant frequency of spoof plasmonic structure for different number of metallic strips N. (c) The far field radiative pattern of the MD emission modified by the spoof plasmonic structure. (d) The radiative (nonradiative) decay rate enhancement as a function of the frequency as a black solid line (red solid line), the blue dash curve corresponds to the extrinsic quantum yield.

DOI: 10.1021/acsanm.8b02318
ACS Appl. Nano Mater. 2019, 2, 1045−1052

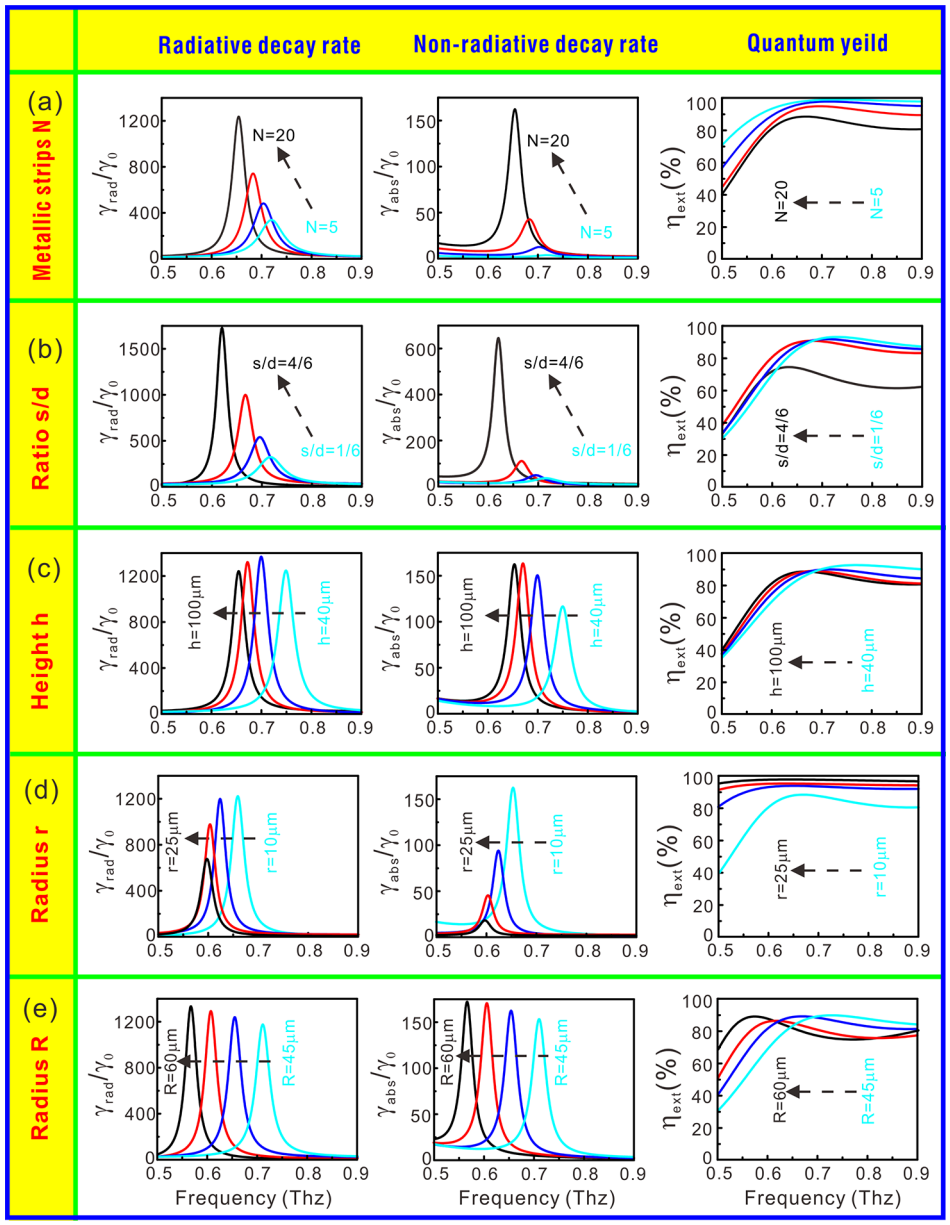

Figure 5. (a–e) Influence of the structural parameters on the radiative decay rate (the first column), nonradiative decay rate (the second column), and quantum yield (the third column) of the MD emission for different numbers of metallic strips *N*, different the ratios *s*/*d*, different heights *h*, different inner radiuses *r*, and different outside radiuses *R*.

plasmonic structure. It can be seen that the radiation pattern is similar to the radiative pattern of bare MD. This result can be attributed to the symmetry of the bare MD mode distribution and the structure in the *x*–*y* plane. It can be desired that the directionality of the far-field radiation be manipulated by breaking the symmetry of the spoof plasmonic structure at the cost of the lower Purcell factor. The directionality of the far-field radiation is the important parameter of a THz source, except for the radiative intensity. Thus, we will study how the far field radiated direction and intensity would change once the structure is tailored in subsequent research work. Furthermore, to characterize the far-field radiated efficiency for introducing the Ohmic losses in metallic material, we also calculate the radiative decay rate factor γ_{rad}/γ_0, nonradiative (absorption) decay rate factor γ_{abs}/γ_0, and the extrinsic quantum yield η_{ext} (black solid line, red solid line, and blue dash line, respectively, in Figure 4d). It can be found that the nonradiative loss increases at the resonant frequency of the spoof plasmonic structure with the increase of far-field radiative power, while the quantum efficiency can be maintained at 88% in this frequency.

In the following, we will discuss how the radiative decay rate, nonradiative decay rate, and the quantum yield change when the structural parameters are changed for varying five parameters: number of metallic strips *N*, the ratio *s*/*d*, height *h*, inner radius *r*, and outside radius *R*. It is vital for guiding the real experimental implementation of the MD emission enhancement by using the spoof plasmonic structure. As can be seen in Figure 5a, the curve of normalized radiative decay rate shifts to lower frequency and peak width becomes narrower, the magnitude becomes larger for increasing the number of metallic strips from $N = 5$ to $N = 20$ as shown in the left figure. Other parameters: outside radius $R = 50$ μm, inner radius $r = 10$ μm, height $h = 100$ μm, and width of metallic

DOI: 10.1021/acsanm.8b02318
ACS Appl. Nano Mater. 2019, 2, 1045–1052

strips $s = 25\pi/9$ μm are used in Figure 5a. It agrees with our above conclusion that the stronger localized magnetic field intensity can further enhance MD emission with increasing the number of metallic strips. At the same time, the normalized nonradiative (absorption) decay rate also increases with the increase of radiative decay rate at the resonant frequency of the spoof plasmonic structure. Particularly, the normalized nonradiative decay rate reaches up to 680 for $N = 20$ at frequency 0.655 THz as shown in the middle figure. Then, we also calculate the extrinsic quantum yield for changing the number of metallic strips of spoof plasmonic structure in the rightmost diagram of Figure 5a. It can be found that the quantum yield drops from 99% to 85% with an increase in the number of metallic strips due to the increase of nonradiative loss. In Figure 2e, we have discussed the influence of the width of metallic strips on the localized magnetic field intensity, and the field intensity can be effectively enhanced by increasing the width. Thus, we also investigate normalized radiative, nonradiative decay rate, and extrinsic quantum yield of the MD emission for different widths of metallic strips in Figure 5b. It can be found that the peak of normalized radiative decay rate shifts from 0.728 THz to 0.63 THz, the magnitude increases from 300 to 1750, and the peak width becomes narrow with tuning the ratio s/d from 1/6 to 4/6. Here, the number of metallic strips is $N = 20$, and other parameters are the same as in Figure 5a. Particularly, the absorptive loss also sharply increases with an increase in the widths of metallic strips. Thus, the quantum yield quickly drops from 93% to 75% for tuning the ratio from 1/6 to 4/6 in Figure 5b. In Figure 5c, we further investigate the evolution of normalized decay rates and quantum yield by changing the height of the spoof plasmonic structure. With an increase in the height of structure from 40 to 100 μm, the peaks of normalized radiative and nonradiative decay rates red-shift to lower frequency, while the magnitude of the peaks do not obviously change with increasing structural height. Thus, the change of the extrinsic quantum yield is also not obvious when the structural height is tuned. Similarly, the frequency and magnitude of the peak can also be tuned freely by changing the inner radius r and outside radius R of the spoof plasmonic structure for height $h = 100$ μm and width of metallic strips $s = 25\pi/9$ μm, as can be seen in Figure 5d and 5e. It is worth noting that the extrinsic quantum yield can maintain a high value for changing the structural parameters at the resonant frequency. The results indicate that the spoof plasmonic structure may provide a new platform to strongly enhanced MD transitions in natural-ion-doped particles such as Er^{3+} and Tm^{3+} in the terahertz frequency.[20,34]

CONCLUSION

In summary, we have proposed a spoof plasmonic structure by simply inserting metallic strips into a hollow Si cylinder to induce a magnetic "hot spot" for the MD emission enhancement. Under the plane wave irradiation, we investigate the influence of structural parameters on the localized magnetic field intensity in a 2D scenario. The results indicated that the intensity could be sharply enhanced with increasing number and width of metallic strips. The ability to strongly focus a magnetic field is a crucial condition for enhancement of the MD emission by modifying the electromagnetic environment around the MD emitter. In this context, we numerically demonstrate that the PF of a MD located at the structural center can be over 10^3, which is 1 order of magnitude larger than the bare hollow Si cylinder. Particularly, the ED emission is suppressed with a PF less than one when the MD emission is strongly enhanced at the frequency of the MD resonance. Furthermore, we also demonstrate that the frequency and magnitude of the peak in the PF spectrum can also be tuned freely by tailoring the outside radius, inner radius, and height of the spoof plasmonic structure. These results may open a novel route for enhancing the MD emission and improve the magnetic light manipulations in the terahertz region.

METHODS

In this paper, the numerical simulations are calculated by using commercial software COMSOL Multiphysics. The calculated region is surrounded by perfectly matched layers to eliminate the undesired reflections. In the calculation of the scattering cross section, the total scattering cross sections of the spoof plasmonic structure are obtained by integrating the normal scattering Poynting vector on a closed curve that encloses the whole structure in a 2D scene. The structure is placed in a vacuum and incident with a TM plane wave (propagation direction perpendicular to structured axis). In the calculation of the PF of the magnetic dipole emission, we put a MD emitter with the magnetic dipole moment parallel to the z-axis in the structural center of the 3D spoof plasmonic structure. Then, the structure is excited by the MD emitter. The normalized far-field radiated power can be obtained by the integral of power flow through a closed surface containing the dipole and the structure, while the absorbed power is calculated by the volume integral of power dissipation in the Cu strips of the spoof plasmonic structure.

AUTHOR INFORMATION

Corresponding Authors

*E-mail: hwwu@aust.edu.cn.
*E-mail: aust47@yahoo.com.

ORCID

Hong-Wei Wu: 0000-0002-0602-3700
Ru-Wen Peng: 0000-0003-0424-2771

Notes

The authors declare no competing financial interest.

ACKNOWLEDGMENTS

This work was supported by the National Key R&D Program of China (2017YFA0303702), the National Natural Science Foundation of China (NSFC) (Grant Nos. 11847002, 51502005, 11804004, 11634005, and 11604143), and Anhui Provincial Natural Science Foundation (Grant No. 1708085QA11 and 1508085QF140).

REFERENCES

(1) Cowan, R. D. *The Theory of Atomic Structure and Spectra*; University of California Press: 1981; Vol. 3.

(2) Soukoulis, C. M.; Wegener, M. Past Achievements and Future Challenges in the Development of Three-Dimensional Photonic Metamaterials. *Nat. Photonics* **2011**, *5*, 523−530.

(3) Staude, I.; Miroshnichenko, A. E.; Decker, M.; Fofang, N. T.; Liu, S.; Gonzales, E.; Dominguez, J.; Luk, T. S.; Neshev, D. N.; Brener, I.; Kivshar, Y. S. Tailoring Directional Scattering through Magnetic and Electric Resonances in Subwavelength Silicon Nanodisks. *ACS Nano* **2013**, *7*, 7824−7832.

(4) Liu, Z.; Liu, G.; Fu, G.; Liu, X.; Wang, Y. Multi-Band Light Perfect Absorption by A Metal Layer-Coupled Dielectric Metamaterial. *Opt. Express* **2016**, *24*, 5020−5025.

(5) Smirnova, D.; Kivshar, Y. S. Multipolar Nonlinear Nanophotonics. *Optica* **2016**, *3*, 1241−1255.

(6) Hussain, R.; Kruk, S. S.; Bonner, C. E.; Noginov, M. A.; Staude, I.; Kivshar, Y. S.; Noginova, N.; Neshev, D. N. Enhancing Eu^{3+}

DOI: 10.1021/acsanm.8b02318
ACS Appl. Nano Mater. 2019, 2, 1045−1052

Magnetic Dipole Emission by Resonant Plasmonic Nanostructures. *Opt. Lett.* **2015**, *40*, 1659−1662.
(7) Karaveli, S.; Zia, R. Spectral Tuning by Selective Enhancement of Electric and Magnetic Dipole Emission. *Phys. Rev. Lett.* **2011**, *106*, 193004.
(8) Choi, B.; Iwanaga, M.; Sugimoto, Y.; Sakoda, K.; Miyazaki, H. T. Selective Plasmonic Enhancement of Electric- and Magnetic-Dipole Radiations of Er Ions. *Nano Lett.* **2016**, *16*, 5191−5196.
(9) Chigrin, D. N.; Kumar, D.; Cuma, D.; Von Plessen, G. Emission Quenching of Magnetic Dipole Transitions near a Metal Nanoparticle. *ACS Photonics* **2016**, *3*, 27−34.
(10) Hein, S. M.; Giessen, H. Tailoring Magnetic Dipole Emission with Plasmonic Split-Ring Resonators. *Phys. Rev. Lett.* **2013**, *111*, 26803.
(11) Rolly, B.; Bebey, B.; Bidault, S.; Stout, B.; Bonod, N. Promoting Magnetic Dipolar Transition in Trivalent Lanthanide Ions with Lossless Mie Resonances. *Phys. Rev. B: Condens. Matter Mater. Phys.* **2012**, *85*, 245432.
(12) Schmidt, M. K.; Esteban, R.; Sáenz, J. J.; Suárez-Lacalle, I.; Mackowski, S.; Aizpurua, J. Dielectric Antennas - A Suitable Platform for Controlling Magnetic Dipolar Emission. *Opt. Express* **2012**, *20*, 13636−13650.
(13) Feng, T.; Xu, Y.; Liang, Z.; Zhang, W. All-dielectric hollow nanodisk for tailoring magnetic dipole emission. *Opt. Lett.* **2016**, *41*, 5011−5014.
(14) Li, J.; Verellen, N.; Van Dorpe, P. Enhancing Magnetic Dipole Emission by a Nano-Doughnut-Shaped Silicon Disk. *ACS Photonics* **2017**, *4*, 1893−1898.
(15) Feng, T.; Zhang, W.; Liang, Z.; Xu, Y.; Miroshnichenko, A. E. Isotropic Magnetic Purcell Effect. *ACS Photonics* **2018**, *5*, 678−683.
(16) Sanz-Paz, M.; Ernandes, C.; Esparza, J. U.; Burr, G. W.; van Hulst, N. F.; Maître, A.; Aigouy, L.; Gacoin, T.; Bonod, N.; Garcia-Parajo, M. F.; Bidault, S.; Mivelle, M. Enhancing Magnetic Light Emission with All Dielectric Optical Nanoantennas. *Nano Lett.* **2018**, *18*, 3481−3487.
(17) Albella, P.; Poyli, M. A.; Schmidt, M. K.; Maier, S. A.; Moreno, F.; Sánez, J. J.; Aizpurua, J. Low-Loss Electric and Magnetic Field-Enhanced Spectroscopy with Subwavelength Silicon Dimers. *J. Phys. Chem. C* **2013**, *117*, 13573−13584.
(18) Bakker, R. M.; Permyakov, D.; Yu, Y. F.; Markovich, D.; Paniagua-Domínguez, R.; Gonzaga, L.; Samusev, A.; Kivshar, Y.; Luk'yanchuk, B.; Kuznetsov, A. I. Magnetic and Electric Hotspots with Silicon Nanodimers. *Nano Lett.* **2015**, *15*, 2137−2142.
(19) Regmi, R.; Berthelot, J.; Winkler, P. M.; Mivelle, M.; Proust, J.; Bedu, F.; Ozerov, I.; Begou, T.; Lumeau, J.; Rigneault, H.; Garcá-Parajó, M. F.; Bidault, S.; Wenger, J.; Bonod, N. All-Dielectric Silicon Nanogap Antennas To Enhance the Fluorescence of Single Molecules. *Nano Lett.* **2016**, *16*, 5143−5151.
(20) Mikhaylovskiy, R.; Huisman, T. J.; Pisarev, R. V.; Rasing, T.; Kimel, A. V. Selective Excitation of Terahertz Magnetic and Electric Dipoles in Er^{3+} Ions by Femtosecond Laser Pulses in $ErFeO_3$. *Phys. Rev. Lett.* **2017**, *118*, 017205.
(21) Pors, A.; Moreno, E.; Martin-Moreno, L.; Pendry, J. B.; Garcia-Vidal, F. J. Localized Spoof Plasmons Arise while Texturing Closed Surfaces. *Phys. Rev. Lett.* **2012**, *108*, 223905.
(22) Shen, X. P.; Cui, T. J. Ultrathin Plasmonic Metamaterial for Spoof Localized Surface Plasmons. *Laser Photonic Rev.* **2014**, *8*, 137−145.
(23) Gao, Z.; Gao, F.; Xu, H.; Zhang, Y.; Zhang, B. Localized Spoof Surface Plasmons in Textured Open Metal Surfaces. *Opt. Lett.* **2016**, *41*, 2181−2184.
(24) Wu, H. W.; Chen, H. J.; Fan, H. Y.; Li, Y.; Fang, X. W. Trapped Spoof Surface Plasmons with Structured Defects in Textured Close Surface. *Opt. Lett.* **2017**, *42*, 791−794.
(25) Gao, Z.; Wu, L.; Gao, F.; Luo, Y.; Zhang, B. Spoof Plasmonics: From Metamaterial Concept to Topological Description. *Adv. Mater.* **2018**, *30*, 1706683.
(26) Liao, Z.; Luo, Y.; Fernández-Domínguez, A. I.; Shen, X.; Maier, S. A.; Cui, T. J. High-Order Localized Spoof Surface Plasmon Resonances and Experimental Verifications. *Sci. Rep.* **2015**, *5*, 9590.
(27) Liao, Z.; Shen, X.; Pan, B. C.; Zhao, J.; Luo, Y.; Cui, T. J. Combined System for Efficient Excitation and Capture of LSP Resonances and Flexible Control of SPP Transmissions. *ACS Photonics* **2015**, *2*, 738−743.
(28) Zhang, J.; Liao, Z.; Luo, Y.; Shen, X.; Maier, S. A.; Cui, T. J. Spoof Plasmon Hybridization. *Laser Photonics Rev.* **2017**, *11*, 1600191.
(29) Huidobro, P. A.; Shen, X.; Cuerda, J.; Moreno, E.; Martin-Moreno, L.; Garcia-Vidal, F. J.; Cui, T. J.; Pendry, J. B. Magnetic Localized Surface Plasmons. *Phys. Rev. X* **2014**, *4*, 021003.
(30) Wu, H. W.; Han, Y. Z.; Chen, H. J.; Zhou, Y.; Li, X. C.; Gao, J.; Sheng, Z. Q. Physical Mechanism of Order between Electric and Magnetic Dipoles in Spoof Plasmonic Structures. *Opt. Lett.* **2017**, *42*, 4521−4524.
(31) Wu, H. W.; Chen, H. J.; Xu, H. F.; Fan, R. H.; Li, Y. Tunable Multiband Directional Electromagnetic Scattering from Spoof Mie Resonant Structure. *Sci. Rep.* **2018**, *8*, 8817.
(32) Wu, H. W.; Wang, F.; Dong, Y. Q.; Shu, F. Z.; Zhang, K.; Peng, R. W.; Xiong, X.; Wang, M. Cavity Modes with Optical Orbital Angular Momentum in A Metamaterial Ring Based on Transformation Optics. *Opt. Express* **2015**, *23*, 32087−32097.
(33) Liao, Z.; Fernández-Domínguez, A. I.; Zhang, J.; Maier, S. A.; Cui, T. J.; Luo, Y. Homogenous Metamaterial Description of Localized Spoof Plasmons in Spiral Geometries. *ACS Photonics* **2016**, *3*, 1768−1775.
(34) Baierl, S.; Hohenleutner, M.; Kampfrath, T.; Zvezdin, A. K.; Kimel, A. V.; Huber, R.; Mikhaylovskiy, R. V. Nonlinear Spin Control by Terahertz-Driven Anisotropy Fields. *Nat. Photonics* **2016**, *10*, 715−718.
(35) Fu, X.; Liu, X.; Zhou, J. Terahertz Spectroscopic Observation of Spin Reorientation Induced Antiferromagnetic Mode Softening in $DyFeO_3$ Ceramics. *Mater. Lett.* **2014**, *132*, 190−192.
(36) Decker, M.; Staude, I.; Shishkin, I.; Samusev, K.; Parkinson, P.; Sreenivasan, V. K. A.; Minovich, A.; Miroshnichenko, A. E.; Zvyagin, A.; Jagadish, C.; Neshev, D. N.; Kivshar, Yu. S. Dual channel spontaneous emission of quantum-dots in magnetic metamaterials. *Nat. Commun.* **2013**, *4*, 2949.

DOI: 10.1021/acsanm.8b02318
ACS Appl. Nano Mater. 2019, 2, 1045−1052